

# Iron Additions Reduce Sulfide Intrusion and Reverse Seagrass (*Posidonia oceanica*) Decline in Carbonate Sediments

Núria Marbà,<sup>1,\*</sup> Maria Ll. Calleja,<sup>1</sup> Carlos M. Duarte,<sup>1</sup> Elvira Álvarez,<sup>2</sup>  
Elena Díaz-Almela,<sup>1</sup> and Marianne Holmer<sup>3</sup>

<sup>1</sup>Institut Mediterrani d'Estudis Avançats (CSIC-UIB), Miquel Marqués 21, 07190 Esporles (Illes Balears), Spain; <sup>2</sup>Direcció General de Pesca, Conselleria d'Agricultura i Pesca, Govern de les Illes Balears, Foners 10, 07006 Palma de Mallorca (Illes Balears), Spain; <sup>3</sup>Institute of Biology, SDU-Odense University, Campusvej 55, 5230 Odense M, Denmark

## ABSTRACT

We conducted a 2-year in situ experiment to test the capacity of iron additions to reverse the decline experienced by a *Posidonia oceanica* meadow colonizing carbonate, iron poor sediment. Iron additions improved the sediment conditions that support seagrass growth by decreasing the sediment sulfide concentration and sulfate reduction rates, and decreased sulfide intrusion into the plants. Iron additions for 2 years did not significantly change survivorship of shoots present at the onset of the experiment, but significantly increased shoot recruitment and survivorship of shoots recruited during the experiment. After 2 years, iron

additions reversed seagrass decline and yielded positive growth rates of shoots relative to control populations where seagrass continued to decline. This research demonstrates that seagrass decline in carbonate sediments may be reversed by targeting critical processes such as sediment sulfide pools and seagrass nutritional status, controlling the functioning of the ecosystem.

**Key words:** carbonate; sulfur; iron additions; sediment; *Posidonia oceanica*; decline; demography; clonal growth.

## INTRODUCTION

Seagrass meadows rank amongst the most valuable ecosystems on Earth for both functions and services (Duarte 2002), but are also amongst the most threatened, with global decline estimated at approximately 1.8%  $y^{-1}$  (Green and Short 2003; Orth and others 2006). Increased organic and nutrient input is recognized generally as the major

cause of worldwide seagrass decline (Duarte 2002; Green and Short 2003; Duarte and others 2005). Excess organic inputs deteriorate sediment conditions that support seagrass growth by stimulating sulfate reduction and production of sulfide that is toxic to seagrasses (Terrados and others 1999; Holmer and others 2003). The effects of sulfides are buffered in iron-rich sediments by the precipitation of pyrite as sulfides combine with iron (Bernier 1984). Seagrasses growing in carbonate sediments are particularly vulnerable to increased organic inputs because the sediments are iron-poor (Duarte and others 1995) and lack sulfide buffering capacity.

Received 18 April 2006; accepted 15 April 2007; published online 20 June 2007.

\*Corresponding author; e-mail: nuria.marba@uib.es

Further, Mediterranean seagrass (*Posidonia oceanica*) meadows growing on carbonate sediments have been reported to continue to decline even after suppression of organic inputs (compare Delgado and others 1999). No intervention has yet been able to stop or reverse *P. oceanica* decline once detected. *P. oceanica* meadows, which represent the dominant and most productive coastal ecosystem in the Mediterranean, are experiencing widespread decline throughout the region, with current decline rates resulting, on average, in a reduction of seagrass density to half in 6.8 years (Marbà and others 2005). Losses of Mediterranean *P. oceanica* meadows are particularly concerning, as the slow clonal growth ( $1\text{--}7\text{ cm y}^{-1}$ , Marbà and Duarte 1998) and sparse reproduction (Pergent and others 1989) of this species results in extraordinarily long recolonization rates (centuries to millenium, Duarte 1995; Marbà and others 2002).

Short-term (1–8 months) iron addition experiments to seagrass sediments have shown a stimulation of seagrass leaf growth (Duarte and others 1995; Chambers and others 2001; Holmer and others 2005), as well as a suppression of sulfate reduction activity in *P. oceanica* sediments receiving excess organic inputs (Holmer and others 2005). These short-term experiments in impacted carbonate sediments, however, have not tested the ability of iron inputs to discontinue or reverse seagrass decline. Here we present the results of a 2-year iron addition experiment testing whether iron additions can increase the resistance of *P. oceanica* meadows to organic inputs by buffering sulfide production and stimulating clonal growth, thereby reversing seagrass decline. The examination of the demographic response to experimental manipulations in *P. oceanica* is particularly challenging, because of the slow recruitment rates and shoot turnover time (less than  $10\% \text{ y}^{-1}$  and up to few decades, respectively, Marbà and others 1996, 2005) characteristic of this species, the slowest-growing seagrass in the world (Marbà and Duarte 1998). In addition, shoot density in *P. oceanica* meadows is heterogeneous as reflected by, on average, a coefficient of variation of 15% (for example, Marbà and others 2005). The slow growth, and to some extent the spatial heterogeneity in *P. oceanica* structure, rules out spectacular demographic responses to any experimental treatment even if imposed over relatively long (2 years) experimental periods, as substantial responses can only be expressed over time scales of decades to centuries.

## METHODS

The experiment was conducted on an impacted *P. oceanica* meadow growing at 17 m depth in Es Port de Cabrera, Cabrera Island, the largest of 19 islands and islets forming the Cabrera Archipelago National Park ( $39^{\circ}8.81'N$   $2^{\circ}55.86'E$ , Balearic Islands, Spanish Mediterranean). Es Port de Cabrera is a sheltered bay traditionally used as a natural harbor. Since the Archipelago was declared a national park in 1991 it hosts the park's visitor center, facilities, and moorings for 50 pleasure boats, and, thus, supports substantial human pressure. The meadow at Es Port de Cabrera has been in decline for the last decade at an average rate exceeding  $4\% \text{ y}^{-1}$  (Marbà and others 2002). The decline of the meadow at Es Port de Cabrera is attributed to enhanced sulfate reduction rates ( $12.5\text{ mmol sulfate m}^{-2} \text{ d}^{-1}$ , Holmer and others 2003) and sulfide accumulation in the sediments. Stable carbon-isotope ratios of bacterial biomarkers identified sedimentary inputs ( $279\text{ mg C m}^{-2} \text{ d}^{-1}$ ) as an important source of organic carbon to support bacterial activity at this site (Holmer and others 2004).

In July 2002 eight experimental  $1.5\text{ m} \times 1.5\text{ m}$  permanent plots were installed in the meadow. The plots were distributed along two rows separated by a 4 m corridor, with neighboring plots within the row separated by 2 m. One permanent  $0.5\text{ m} \times 0.5\text{ m}$  quadrat, for seagrass shoot census, was delimited at the center of each plot, where sampling of plants and sediments was prevented for the entire duration of the experiment. The top 30 cm sediment layer of the 4 plots along 1 row were enriched with iron pulses of  $0.8\text{ mol iron m}^{-2}$ , as Fe-chelate (Fe-EDDHA) dissolved in seawater, comparable to the inputs in previous iron addition experiments to seagrass sediments (Holmer and others 2005), in July 2002, November 2002, July 2003, and March 2004. Iron pulses were applied through 49 injections of 60 ml Fe-chelate dissolved in seawater per plot, where 5 ml of solution per injection were added at the top 5, 10, 15, 20, 25, and 30 cm of sediment. The other four plots were kept as controls. The plots were visited every fourth month over 2 years.

At each visit, SCUBA divers collected two sediment cores per experimental plot, one of internal diameter (i.d.) 2.6 cm and one of i.d. 4.3 cm. The depth of all sediment cores was 10 cm, and cutting of roots and rhizomes was avoided during the collections. The sediment collected in the 2.6 cm diameter cores was used to measure the sediment sulfate reduction rate (SRR), acid volatile sulfides

(AVS) and chromium reducible sulfur (CRS). The sediment collected in the 4.3 cm diameter cores was used for measuring pore-water concentrations of sulfate, sulfides and total dissolved iron ( $\text{Fe}^{2+} + \text{Fe}^{3+}$ ) and the solid phase characteristics (sediment density, water content, porosity and organic matter content). During visits when iron pulses were supplied to the Fe-enriched plots, all sediment cores were collected prior to iron additions. In addition, at the beginning of the experiment one sediment core per plot was collected immediately after iron injections to assess the increase in iron concentration resulting from the injections.

Sulfate reduction rates were quantified by the core-injection technique (Jørgensen 1978). Two microliters of  $^{35}\text{S}$ -sulfate (70 kBq) were injected with 1-cm intervals through predrilled silicone filled holes and the cores were incubated at in situ temperature in darkness for 1–3 h. After the incubation, the sediment was fixed in 1 M zinc acetate (vol:vol). The samples were stored frozen until distillation according to the two-step extraction scheme; in the first step AVS was liberated by the addition of 6 M HCl (in 50% ethanol) and in the second step CRS was extracted by adding 1 M  $\text{CrCl}_2$  (in 0.5 HCl), both were trapped in zinc acetate, following Fossing and Jørgensen (1989). Radioactivity was counted on a Beckman LS-3801 scintillation counter. Sulfate reduction rates (SRR, in  $\text{nmol SO}_4^{2-} \text{m}^{-3} \text{d}^{-1}$ ) were calculated for each sediment core following Fossing and Jørgensen (1989) as:

$$\text{SRR} = \frac{a}{(a + A)t} \times [\text{SO}_4^{2-}] \times 1.06$$

where  $a$  is the total radioactivity in the traps,  $A$  is the total radioactivity of the sulfate pool after incubation,  $t$  is the incubation time (in days),  $[\text{SO}_4^{2-}]$  is the sulfate concentration in the sediment ( $\text{nmol cm}^{-3}$ ) and 1.06 is the correction factor for microbial isotope fractionation between  $^{32}\text{S}$  and  $^{35}\text{S}$ . The concentrations of reduced sulfide pools from the traps were determined spectrophotometrically according to Cline (1969).

Porewater samples were obtained from sediment cores sliced under  $\text{N}_2$  atmosphere to keep them anoxic. The sediment was centrifuged and supernatant was sampled for analysis of sulfate ( $\text{SO}_4^{2-}$ ), sulfides ( $\text{H}_2\text{S}$ ), and porewater total dissolved iron ( $\text{Fe}^{2+} + \text{Fe}^{3+}$ ). Sulfate was determined using the turbidimetric assay described by Tabatabai (1974). Sulfides were kept in zinc acetate and determined spectrophotometrically according to Cline (1969) and total dissolved iron was kept on HCl (pH 1) and

analyzed as  $\text{Fe}^{2+}$  after addition of hydroxylamine for reduction of  $\text{Fe}^{3+}$  as described by Stookey (1970). Sediment density was obtained by weight of a known volume, and the water content was obtained after drying it overnight at  $105^\circ\text{C}$ . Porosity was calculated from sediment density and water content. Organic matter content was obtained by ignition of the dried sediment overnight at  $450^\circ\text{C}$ .

At the end of the experimental period one sediment core (i.d. 2.6 cm) from each plot was collected to determine the  $\delta^{34}\text{S}_{\text{sulfide}}$  values in the AVS and CRS pools. The sediment (0–10 cm) was distilled as described above according to Fossing and Jørgensen (1989), but the trap content was exchanged with  $\text{AgNO}_3$  solution. The sulfides precipitated in the traps and  $\text{Ag}_2\text{S}$  was collected on a GF/F filter. The  $\delta^{34}\text{S}_{\text{sulfide}}$  value was determined as described below for the plants.

Seagrass shoot demographic parameters were quantified by direct shoot census in the  $0.5 \text{ m} \times 0.5 \text{ m}$  quadrats installed inside the experimental plots following the procedures described in Short and Duarte (2001). At the beginning of the experiment, all shoots within the quadrats were tagged, with a plastic cable tie, and counted. Every eighth and every fourth month during the first and second year, respectively, the number of surviving shoots (that is, shoots tagged with a cable tie) and the number of recruited shoots between consecutive visits (that is, young untagged shoots) in each permanent quadrat were counted. The number of rhizome apexes in the quadrats was also recorded, and the recruited shoots found were tagged with a cable tie of a different color, allowing monitoring of survival of the different shoot cohorts. Identification of rhizome apexes in the permanent plots required minor sediment disturbance during visits. Rhizome apexes of *P. oceanica* were easy to identify visually, as they had shorter and more curved leaf shoots than those on vertical rhizomes. Occasionally, rhizome apexes were identified by carefully touching them by hand within the top 0–2 cm sediment layer. These measurements provided estimates of shoot and apex density, survival trajectories for shoots older than 2 years and shoot cohorts recruited during the experiment, curves of cumulative recruitment during the experiment, and the absolute and specific rates of shoot mortality, recruitment and population growth in between consecutive visits. Absolute and relative shoot mortality, recruitment and net population growth rates were estimated as described in Marbà and others (2005).

Leaf and horizontal rhizome elongation rates (in  $\text{cm shoot}^{-1} \text{y}^{-1}$  and  $\text{cm rhizome apex}^{-1} \text{y}^{-1}$ ,

respectively) were measured using marking techniques, as described in Short and Duarte (2001), whereas estimates of vertical rhizome growth were quantified retrospectively (Duarte and others 1994) on three shoots of each plot harvested at the end of the experiment. Leaf growth was estimated in between consecutive visits on eight shoots per experimental plot. The horizontal rhizome elongation rate was only estimated during the second year. In July 2003, 14 rhizome apices distributed amongst the 0.5 m × 0.5 m quadrats were tagged with a cable tie, and were harvested at the end of the experiment. Leaf annual production (in g DW m<sup>-2</sup> y<sup>-1</sup>) was estimated as annual leaf elongation rate multiplied by the specific leaf weight (g DW cm leaf<sup>-1</sup>) and shoot density. Similarly, vertical (and horizontal) rhizome annual production (in g DW m<sup>-2</sup> y<sup>-1</sup>) was calculated as the product of annual vertical (and horizontal) rhizome elongation rate, specific vertical (and horizontal) rhizome weight (g DW cm rhizome<sup>-1</sup>) and shoot (and apex) density.

Iron concentration, δ<sup>34</sup>S abundance and the fraction of total sulfur in plant tissues (that is, leaves, rhizomes, roots) derived from sedimentary sulfides were measured on *P. oceanica* samples collected from each experimental plot at the end of the experiment. Sulfur isotope analyses were made by the National Isotope Geosciences Facility (Nottingham, UK) using an automated, on-line facility coupled to a Thermo Finnigan Delta XL. The sulfur isotope composition of a sample is expressed in the standard δ notation given by:

$$\delta^{34}\text{S} = \frac{[(R_{\text{sample}}/R_{\text{standard}}) - 1]}{1000}$$

where  $R = {}^{34}\text{S}/{}^{32}\text{S}$ . Values are expressed on a per mil (‰) basis and were calibrated to CDT (troilite standard from the Canyon Diablo meteorite) using IAEA standards S1 and S2. Replicate analyses of internal standards (barium sulfate, silver sulfide and an internal laboratory organic standard, broccoli) showed that reproducibility was ±0.4‰ or better. To determine the relative contribution of sediment sulfide to the sulfur composition in the leaves, rhizomes and roots, the fraction of the total sulfur pool derived from sedimentary sulfides ( $F_{\text{sulfide}}$ ) was estimated:

$$F_{\text{sulfide}} = \frac{\delta^{34}\text{S}_{\text{tissue}} - \delta^{34}\text{S}_{\text{sulfate}}}{\delta^{34}\text{S}_{\text{sulfide}} - \delta^{34}\text{S}_{\text{sulfate}}}$$

where δ<sup>34</sup>S<sub>tissue</sub> is the value measured in the leaf, rhizome or root, δ<sup>34</sup>S<sub>sulfate</sub> was the values measured in the seawater (average +20.99‰) and δ<sup>34</sup>S<sub>sulfide</sub>

was the values measured in the sedimentary AVS pools (average -17.15‰).

Iron concentration in plant tissues was obtained after acid hydrolysis (1 M HCl) for 1 h at 105°C and analyzed as described above for Fe<sup>2+</sup>.

Sediment and plant responses to iron additions, per sampling visit and per grand mean (that is, average across the entire experiment duration), were examined using Student's *t* test. Similarly, Student's *t* test was used to assess the changes in sediment parameters between the beginning and end of the experiment. The persistence of consistent responses of sediment parameters to iron additions during the experiment was identified using Wilcoxon's signed-ranks test. The temporal trend of plant responses to iron additions was evaluated using regression analysis on log transformed variables, and differences between treatments by comparing the slopes using Student's *t*-test. Standard errors of mean values are always provided.

## RESULTS

No significant differences (*t*-test,  $P > 0.05$ ) among bulk sediment parameters (that is, sediment density, porosity and organic carbon content) between control versus iron-enriched plots either initially or after 1 year of measurement were observed (Table 1).

The sediments investigated were iron poor, with porewater total dissolved iron in control plots averaging  $0.72 \pm 0.16$  mmol Fe m<sup>-2</sup> (range 0.29–1.41 mmol Fe m<sup>-2</sup>, Table 1) during the experiment. Iron additions raised the amount of porewater total dissolved iron three-orders of magnitude following injections ( $808 \pm 526$  mmol Fe m<sup>-2</sup>, Table 1), but these declined rapidly, likely through diffusive loss and benthic irrigation, to average  $1.75 \pm 0.59$  mmol Fe m<sup>-2</sup> 8 months following injections (Table 1). Despite the losses, iron injections maintained elevated porewater total dissolved iron levels twofold above that in control plots, at least 8 months following injections. The amount of porewater total dissolved iron in iron-enriched plots was maintained significantly (Wilcoxon's test,  $P < 0.05$ ) higher than that in control plots for the entire duration of the experiment. The porewater sulfide concentration in control plots increased greatly, but not significantly (*t*-test,  $P > 0.05$ ), during the study, from low initial concentrations of  $0.42 \pm 0.12$  mmol H<sub>2</sub>S m<sup>-2</sup> at the onset of the experiment to reach concentrations of  $5.82 \pm 3.66$  mmol H<sub>2</sub>S m<sup>-2</sup> by the end of the experiment (Table 1). The iron-enriched sediments

**Table 1.** Average (and standard error, n = 4) Sediment Density, Porosity, Organic Carbon Content, Porewater Total Dissolved Fe, H<sub>2</sub>S Pool, Sulfate Reduction Rate (SRR), and Acid Volatile Sulfide (AVS), Chromium Reducible Sulfur (CRS) and Total Reducible Sulfide (TRS) Pools, within the Top 10 cm Sediment Layer, in Fe-Enriched and Control Plots during Experiment Visits

Parameter	Treatment	July 2002	November 2002	March 2003	July 2003	November 2003	April 2004	July 2004	Average ± SE
Sediment density (g cm <sup>-3</sup> )	Fe-enriched	1.38 ± 0.01	1.39 ± 0.04	1.37 ± 0.01					1.38 ± 0.01
	Control	1.39 ± 0.02	1.35 ± 0.02	1.38 ± 0.03					1.37 ± 0.01
Porosity (g H <sub>2</sub> O cm <sup>-3</sup> )	Fe-enriched	0.72 ± 0.02	0.70 ± 0.02	0.67 ± 0.03					
	Control	0.72 ± 0.03	0.73 ± 0.02	0.72 ± 0.03					
Organic carbon content (g m <sup>-2</sup> )	Fe-enriched	4,657 ± 175	4,469 ± 202	4,486 ± 123					4537 ± 73
	Control	4,801 ± 82	4,683 ± 153	4,535 ± 149					4,672 ± 94
Total dissolved Fe (mmol m <sup>-2</sup> )	Fe-enriched	808 ± 526*	3.13 ± 0.96	2.19 ± 1.19	1.18 ± 0.28	2.30 ± 1.13	1.49 ± 0.59	0.80 ± 0.46	1.85 ± 0.38
	Control	0.49 ± 0.19	0.29 ± 0.05	1.41 ± 0.13	0.74 ± 0.03	1.02 ± 0.31	0.71 ± 0.39	0.36 ± 0.05	0.72 ± 0.16
H <sub>2</sub> S (mmol m <sup>-2</sup> )	Fe-enriched	0.33 ± 0.18	1.28 ± 1.09	0.22 ± 0.01	2.68 ± 1.01	1.43 ± 0.38	0.28 ± 0.03	1.21 ± 0.45	1.06 ± 0.36
	Control	0.42 ± 0.12	0.35 ± 0.13	0.27 ± 0.07	1.16 ± 0.68	1.82 ± 1.42	0.56 ± 0.27	5.82 ± 3.66	1.49 ± 0.81
SRR (mmol S m <sup>-2</sup> d <sup>-1</sup> )	Fe-enriched	13.47 ± 2.60	8.91 ± 2.85	3.94 ± 1.14	18.38 ± 13.79	4.99 ± 2.05	8.63 ± 0.45	6.27 ± 1.13	9.22 ± 2.09
	Control	19.20 ± 5.50	6.45 ± 0.68	12.00 ± 6.93	4.12 ± 0.28	4.30 ± 1.89	8.12 ± 6.60	11.96 ± 5.39	9.45 ± 2.20
AVS (mol S m <sup>-2</sup> )	Fe-enriched	0.37 ± 0.08	0.43 ± 0.02	0.45 ± 0.15	0.37 ± 0.02	0.37 ± 0.02	0.34	0.32 ± 0.03	0.38 ± 0.02
	Control	0.51 ± 0.11	0.39 ± 0.23	0.41 ± 0.11	0.38 ± 0.01	0.38 ± 0.02	0.30 ± 0.02	0.32 ± 0.01	0.39 ± 0.03
CRS (mol S m <sup>-2</sup> )	Fe-enriched	0.25 ± 0.01	0.22 ± 0.03	0.20 ± 0.01	0.26 ± 0.03	0.27 ± 0.02	0.29	0.32 ± 0.03	0.26 ± 0.02
	Control	0.25 ± 0.02	0.18 ± 0.02	0.17 ± 0.03	0.31 ± 0.01	0.23 ± 0.08	0.26 ± 0.01	0.26 ± 0.01	0.24 ± 0.02
TRS (mol S m <sup>-2</sup> )	Fe-enriched	0.62 ± 0.09	0.65 ± 0.01	0.65 ± 0.15	0.64 ± 0.04	0.64 ± 0.04	0.62	0.64 ± 0.05	0.64 ± 0.01
	Control	0.76 ± 0.11	0.58 ± 0.25	0.55 ± 0.14	0.69 ± 0.02	0.61 ± 0.07	0.56 ± 0.01	0.58 ± 0.01	0.62 ± 0.03

Total dissolved Fe in Fe-enriched plots in July 2002 (asterisks) was measured after iron injections. Average (and standard error; n = 7, except for sediment density, porosity, organic carbon content n = 3, and porewater total dissolved Fe n = 6) estimates across the entire duration of the experiment in Fe-enriched and control plots are also provided. Standard error of average values are not provided when n = 1.

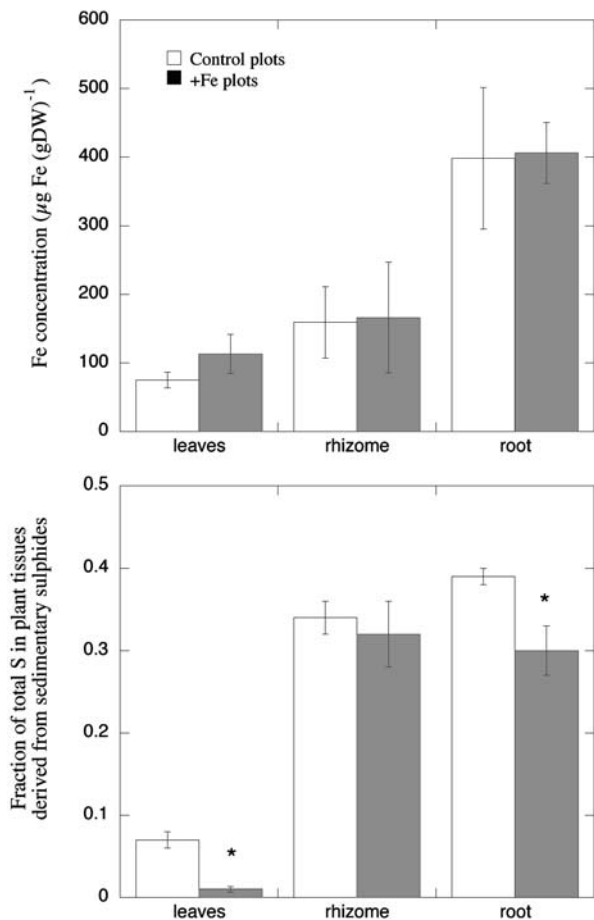


**Figure 1.** The average ( $\pm$ SE) iron concentration and the fraction of total sulfur ( $F_{\text{sulfide}}$ ) in leaves, rhizomes and roots derived from sedimentary sulfides (AVS pool) in control (empty bars) and Fe-enriched (grey bars) experimental plots. The average iron concentrations in leaves was computed as the average of seven sampling events during the experiment ( $n = 28$ ), whereas the rest of the parameters were estimated at the end of the experiment. Statistically significant differences ( $t$ -test,  $P < 0.05$ ) between treatments are indicated (asterisks).

did not show such an increase of porewater sulfide concentration during the experiment (Table 1). Despite the wide temporal fluctuations in porewater sulfide concentration in control and iron-enriched sediments (Table 1), the average porewater sulfide concentration during the entire study was 40% higher in control plots ( $1.49 \pm 0.81 \text{ mmol H}_2\text{S m}^{-2}$ , Table 1) than in iron-enriched ones ( $1.06 \pm 0.46 \text{ mmol H}_2\text{S m}^{-2}$ , Table 1).

Sediment sulfate reduction rates fluctuated widely over time in iron-enriched and control plots, the highest rates being observed during spring–summer (Table 1). However, similar ( $t$ -test,  $P > 0.05$ ) sediment sulfate reduction rates were

observed at the onset and end of the experiment in control plots (Table 1). Conversely, 2 years of iron additions significantly ( $t$ -test,  $P < 0.05$ ) decreased sediment sulfate reduction rates by twofold (Table 1). Total pools of reduced sulfides (TRS) were similar in sediments of fertilized and control plots, averaging  $0.63 \pm 0.004 \text{ mol S m}^{-2}$  in iron-enriched plots and  $0.62 \pm 0.03 \text{ mol S m}^{-2}$  in control plots (Table 1). As a result, the turnover rate of total reduced sulfides in the iron-enriched plots was half of that in the control plots at the end of the experiment, indicating lower oxygen consumption for re-oxidation of sulfides. In addition, the total sulfur pools shifted over the last year of the experiment, in response to iron additions, towards a slightly greater contribution of CRS (pyrite, 47% in the iron-enriched plots, compared to an average of 41% in the control plots by the end of the experiment, Table 1).

The iron concentration in tissues of control plants was very low, with leaves having the lowest iron concentrations (Figure 1). Iron concentration in seagrass leaves tended to increase, although not significantly ( $t$ -test,  $P > 0.05$ ), in response to Fe additions, with the average Fe concentration increasing from  $75.1 \pm 11.5 \mu\text{g Fe (g DW)}^{-1}$  in control plants to an average of  $113.4 \pm 28.3 \mu\text{g Fe (g DW)}^{-1}$  in iron-enriched plots during the experiment (Figure 1). Iron concentrations were similar ( $t$ -test,  $P > 0.05$ ) in roots and rhizomes at Fe-enriched and control plots (Figure 1). The  $^{34}\text{S}$  abundance varied across *P. oceanica* tissues of plants in control plots (Table 2). At the end of the experiment, the  $^{34}\text{S}$  abundances in leaves and roots of iron-enriched plots were significantly ( $t$ -test,  $P < 0.05$ ) higher than those in similar tissues of plants growing in control plots (Table 2). Examination, through the  $^{34}\text{S}$  abundance, of the fraction of sedimentary sulfide in the S pool of the seagrasses showed a major (fivefold) and significant ( $t$ -test,  $P < 0.05$ ) reduction in the contribution of sulfide to the S pool of leaves in iron-enriched plots (Figure 1). The contribution of sulfide to the S pool of roots was also significantly ( $t$ -test,  $P < 0.05$ ) lower in plants in iron-enriched than in control plots (Figure 1).

The shoot density declined during the experiment, with an average net decline of 11.2% (Figure 2), resulting in an average ( $\pm$ SE) specific population growth rate of  $-5.6 \pm 3.8\% \text{ y}^{-1}$  (Table 3). Most of the decline occurred over the first 8 months of the experiment (Figure 2). Iron additions did not result in a significant ( $t$ -test,  $P > 0.05$ ) reduction in shoot mortality of the entire shoot population but they increased significantly ( $t$ -test,

**Table 2.** Average Values of  $\delta^{34}\text{S}$  in *Posidonia oceanica* Leaves, Rhizomes and Roots from Iron-Enriched and Control Plots at the End of the Experiment

Seagrass tissue	Treatment	$\delta^{34}\text{S}$ (‰)	P
Shoot	Iron enriched	20.45 ± 0.14	*
	Control	18.15 ± 0.37	
Rhizome	Iron enriched	8.73 ± 1.42	n.s.
	Control	7.94 ± 0.72	
root	Iron enriched	9.54 ± 0.98	*
	Control	6.29 ± 0.23	

Standard error of average  $\delta^{34}\text{S}$  in shoots, rhizomes, and roots are provided ( $n = 4$ ). The level of significance [ $t$ -test,  $P < 0.05$ (\*);  $P > 0.05$  (NS)] of tissue  $\delta^{34}\text{S}$  signature response to iron additions is indicated.

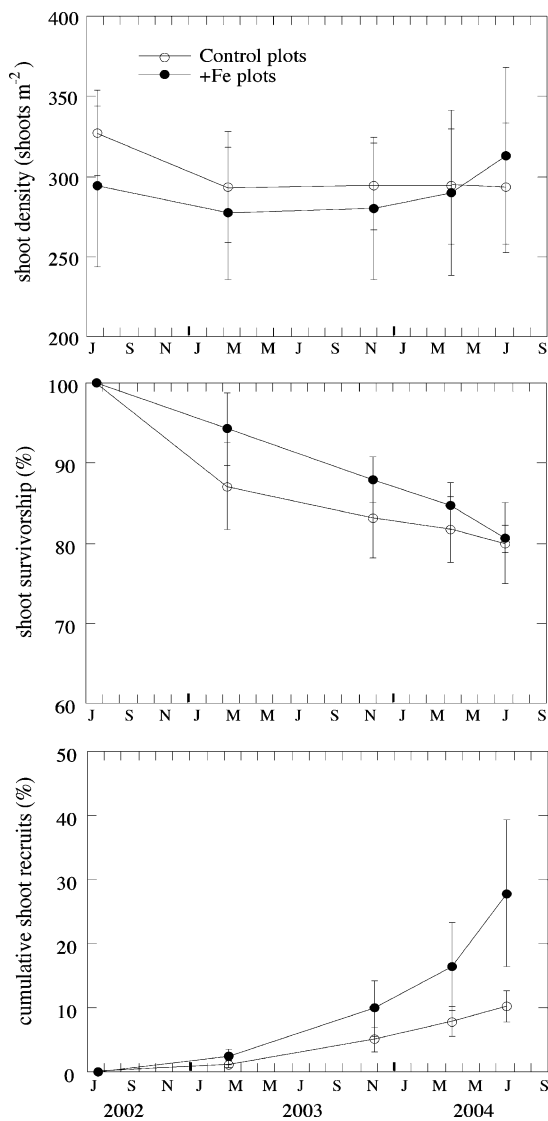


**Figure 2.** Average ( $\pm$ SE;  $n = 4$ ) shoot density, and trajectories (as % of the initial shoot density) of relative shoot survival and cumulative recruitment in control and Fe-enriched experimental plots during the experiment.

$P < 0.05$ ) by 2.5 fold shoot recruitment during the experimental period (Figure 2; Table 3). The average specific recruitment rate in iron-enriched plots increased significantly (regression analysis,  $P < 0.01$ ,  $n = 4$ ) over time, whereas shoots recruited at similar (regression analysis,  $P > 0.5$ ,  $n = 4$ ) average rates in control plots during the experiment. Iron additions did not change survival of shoots present in the meadow at the onset of the experiment; depletion curves were similar ( $t$ -test on the slopes,  $P > 0.05$ ) in iron-enriched and control plots (Figure 2). Conversely, iron additions significantly increased survival of shoots recruited during the experiment (Figure 3). Annual survival of recruits was not significantly different from 100% (regression analysis,  $P > 0.05$ ,  $n = 9$ ) in iron-enriched plots, whereas annual survival of recruits significantly declined to 68% (regression analysis,  $P < 0.01$ ,  $n = 9$ ) in control plots (Figure 3). As a result of these combined responses, iron additions tended to reverse the decline of the meadow toward the end of the experiment, with an increase in shoot density by 7.6% (Figure 4). Responses of shoot population growth rates to iron additions during the experiment were not statistically ( $t$ -test,  $P > 0.05$ , Table 3) significant, due to the large error imposed by the patchiness of the meadow. Examination of temporal trends revealed a significant (regression analysis,  $P < 0.05$ ,  $n = 4$ ) increase in the average shoot population growth rate in iron-enriched plots, whereas no temporal changes were observed (regression analysis,  $P > 0.5$ ,  $n = 4$ ) in control plots.

The increased shoot recruitment in iron-enriched plots was sustained by stimulation, although not significant ( $t$ -test,  $P > 0.05$ ), of clonal growth. In iron-enriched plots, the number of rhizome apices increased (Figure 5), indicative of an increased branching rate, and the rhizome elongation rate tended to be twice that in control plots. The cal-

**Table 3.** Average (and Standard error,  $n = 4$ ) Absolute and specific Shoot Recruitment, Mortality and Population Growth Rates in Fe-Enriched and Control Plots during Experiment Samplings.

Parameter	Treatment	March 2003	November 2003	April 2004	July 2004	Average $\pm$ SE	P
Absolute recruitment rate (shoots $m^{-2} d^{-1}$ )	Fe-enriched control	0.03 $\pm$ 0.02	0.08 $\pm$ 0.03	0.16 $\pm$ 0.11	0.31 $\pm$ 0.11	0.15 $\pm$ 0.07	<0.05
Absolute mortality rate (shoots $m^{-2} d^{-1}$ )	Fe-enriched control	0.02 $\pm$ 0.01	0.05 $\pm$ 0.02	0.07 $\pm$ 0.03	0.08 $\pm$ 0.04	0.06 $\pm$ 0.02	0.81
Absolute population growth rate (shoots $m^{-2} d^{-1}$ )	Fe-enriched control	0.11 $\pm$ 0.07	0.08 $\pm$ 0.02	0.09 $\pm$ 0.04	0.07 $\pm$ 0.03	0.09 $\pm$ 0.01	0.06
Specific recruitment rate (% $d^{-1}$ )	Fe-enriched control	0.16 $\pm$ 0.08	0.05 $\pm$ 0.03	0.06 $\pm$ 0.04	0.09 $\pm$ 0.02	0.06 $\pm$ 0.08	<0.05
Specific mortality rate (% $d^{-1}$ )	Fe-enriched control	-0.07 $\pm$ 0.05	0.01 $\pm$ 0.04	0.07 $\pm$ 0.07	0.22 $\pm$ 0.11	-0.04 $\pm$ 0.04	0.79
Specific population growth rate (% $d^{-1}$ )	Fe-enriched control	-0.14 $\pm$ 0.08	0.00 $\pm$ 0.03	0.01 $\pm$ 0.07	-0.01 $\pm$ 0.06	0.05 $\pm$ 0.02	0.07
	Fe-enriched control	0.01 $\pm$ 0.01	0.03 $\pm$ 0.01	0.05 $\pm$ 0.03	0.10 $\pm$ 0.04	0.02 $\pm$ 0.01	
	Fe-enriched control	0.01 $\pm$ 0.00	0.02 $\pm$ 0.01	0.02 $\pm$ 0.01	0.03 $\pm$ 0.01	0.03 $\pm$ 0.01	
	Fe-enriched control	0.03 $\pm$ 0.02	0.03 $\pm$ 0.01	0.03 $\pm$ 0.01	0.03 $\pm$ 0.01	0.03 $\pm$ 0.01	
	Fe-enriched control	0.06 $\pm$ 0.03	0.02 $\pm$ 0.01	0.02 $\pm$ 0.02	0.03 $\pm$ 0.01	0.03 $\pm$ 0.01	
	Fe-enriched control	-0.02 $\pm$ 0.02	0.00 $\pm$ 0.01	0.02 $\pm$ 0.02	0.08 $\pm$ 0.04	0.02 $\pm$ 0.02	
	Fe-enriched control	-0.05 $\pm$ 0.03	0.00 $\pm$ 0.01	0.00 $\pm$ 0.03	-0.01 $\pm$ 0.02	-0.02 $\pm$ 0.01	

Average (and standard error,  $n = 20$ ) estimates across the entire duration of the experiment in Fe-enriched and control plots are also provided, and the probability of significant differences (Student's *t*-test) between treatments is provided

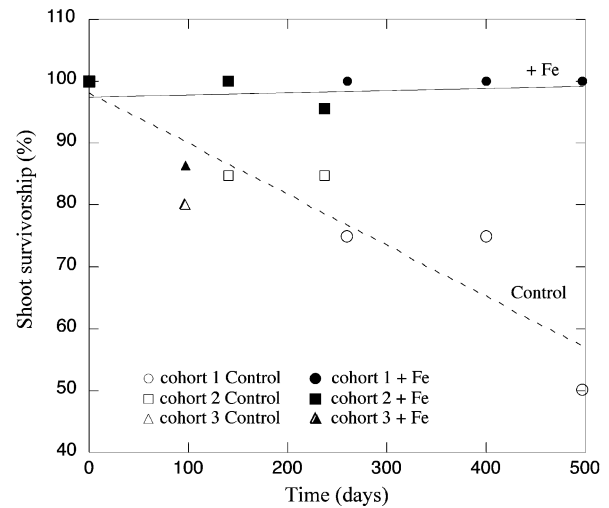


**Figure 3.** Survival of different cohorts of shoots recruited during the experiment in control (*white symbols*) and Fe-enriched (*black symbols*) experimental plots. Survival was calculated as percentage of the total number of shoots per cohort recruited per treatment. The number of shoots recruited in control and enriched plots in cohort 1 (*circles*) was 4 and 8, respectively; in cohort 2 (*squares*) 13 and 22 respectively; in cohort 3 (*triangles*) 10 and 22, respectively. The slopes  $\pm$  SE of fitted depletion equations in control (*dashed line*) and iron-enriched (*solid line*) plots were  $-0.08 \pm 0.01$  shoots  $d^{-1}$  (regression analysis,  $P < 0.0005$ ,  $n = 9$ ) and  $0.003 \pm 0.009$  shoots  $d^{-1}$  (regression analysis,  $P > 0.05$ ,  $n = 9$ ), respectively.

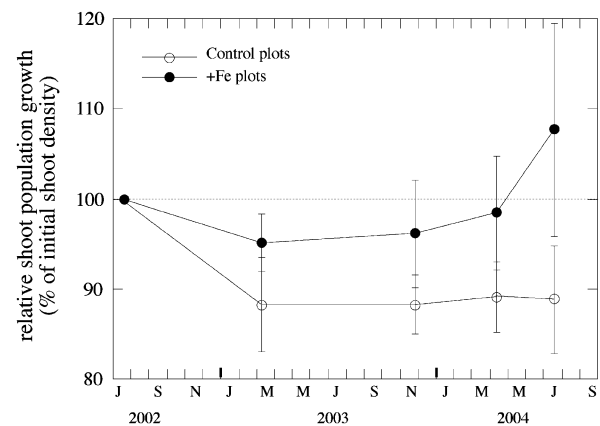


**Figure 4.** Average ( $\pm$ SE;  $n = 4$ ) relative shoot population growth (as % of the initial shoot density) during the experiment in control and iron-enriched plots.

culated average net production rate increased in iron-enriched plots relative to control plots for the net production of horizontal rhizomes (Figure 6), with the total (rhizome + leaf) net production in



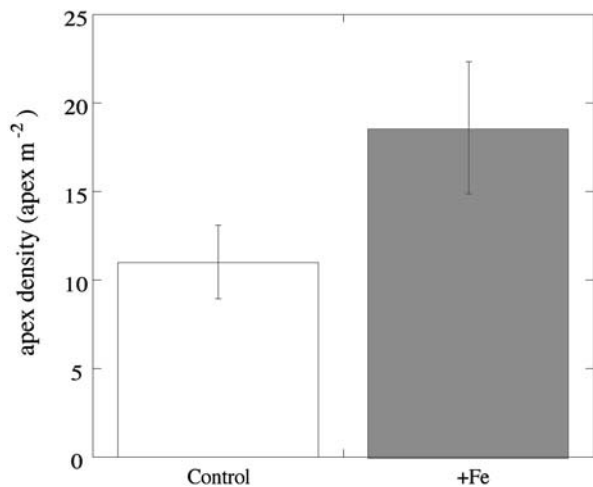


Figure 5. Average ( $\pm$ SE;  $n = 20$ ) density of horizontal rhizome apices in control and iron-enriched plots during the experiment.

iron-enriched plots increasing marginally (7.5% on average) relative to that of control plots during the experiment (Figure 6).

## DISCUSSION

The ecosystem studied was iron-poor, with iron concentrations in seagrass leaves below the critical values ( $100 \mu\text{g Fe (g DW)}^{-1}$ , Duarte and others 1995), the lowest yet reported for *Posidonia oceanica*, and comparable to the lowest values, characteristic of Fe-deficient plants, reported for seagrasses elsewhere (Duarte and others 1995). This iron deficiency renders this ecosystem highly vulnerable to increased organic inputs from emissions of visitors to the Bay, and have been identified as the cause for the severe decline of the meadow (Marbà and others 2002; Holmer and others 2003). The accumulation of toxic sulfides in the sediments, which diffuse into plant tissues as reflected in the  $\delta^{34}\text{S}$  isotope signals in plant tissues, compound with iron-limitation of plant growth to yield the observed seagrass decline (Holmer and others 2005). Seagrass decline, in turn, might contribute to increased sediment sulfide accumulation, because, as the meadow thins, the amount of photosynthetic oxygen released by roots (Borum and others 2006) and, thus, the capacity of the system to reoxidize sediment sulfide would decrease. Experimental iron additions maintained elevated iron pools over 2 years, significantly decreased sediment sulfate reduction rates and tended to reduce sulfide pools, and thus released sulfide pressure on the plants. As a result of these effects, the leaves and roots

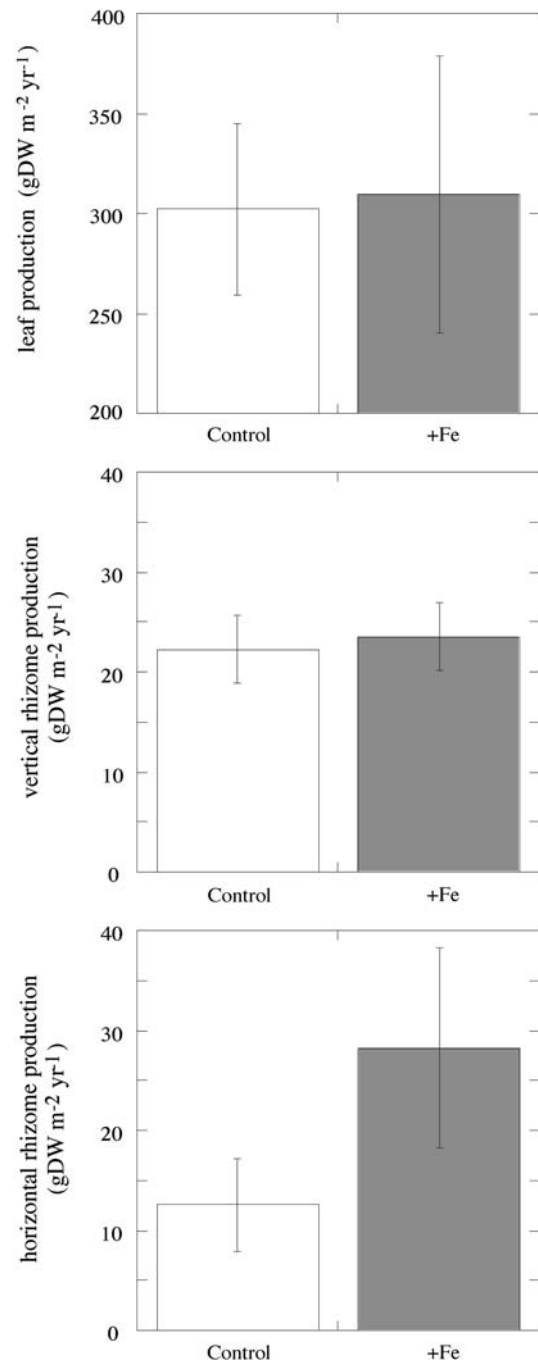


Figure 6. Average ( $\pm$ SE) net leaf and rhizome production in control and iron-enriched plots during the experiment.

showed a significant decrease in sulfide intrusion, as reflected in changes in  $\delta^{34}\text{S}$  isotopic composition in iron-enriched plants, which contributed to accelerate clonal growth. Iron is involved in key sediment and organism processes. Iron is an essential nutrient for plant metabolism. At the same time, iron modulates key ecosystem pro-

cesses, such as pyrite formation, which is a mechanism for removal of sulfides from sediments, thereby decreasing the likelihood of sulfide toxicity. Pyrite formation, moreover removes feed back processes between anoxic conditions and increasing sulfate reduction, which in turn releases sulfides acting as O<sub>2</sub> sinks, that act to preserve anoxic conditions in iron-poor sediments (Chambers and others 2001; Holmer and others 2003, 2005).

Increased clonal growth of *P. oceanica* in response to iron additions confirms the key role of iron in plant nutrition, and as a factor alleviating stress from increased organic inputs and associated high sulfide production (Holmer and others 2003, 2005). Iron additions had previously been shown to stimulate seagrass growth on carbonate sediments in the Caribbean (compare Duarte and others 1995), Florida Bay (Chambers and others 2001) and the Mediterranean meadow studied here (Holmer and others 2005). However, all of these studies were conducted over time scales too short to assess demographic responses, such as those observed here. An increase in shoot recruitment and net population growth of *Posidonia oceanica* in response to 2 years of iron additions represents the first demonstration that iron addition can improve the status of seagrass populations. This observation is particularly remarkable provided the exceedingly slow demographic dynamics of this species (for example, shoot turnover time in the control plots  $23.3 \pm 8.2$  years), where direct observation is challenging (Marbà and others 2005).

Most importantly, the results presented here demonstrate that sustained iron additions can reverse seagrass decline, as the meadow shifted from declining by about  $7\% \text{ y}^{-1}$  to expanding at a rate of  $7\% \text{ y}^{-1}$  as a result of iron additions. This shift was possible because of the stimulation of rhizome growth, which is the basis for clonal growth, resulting in a sizeable increase in the recruitment rate. Despite no significant reduction in bulk shoot mortality in response to iron additions, the increase in shoot recruitment rate sufficed to drive the population from net decline to net growth. The observation that the mortality rate of new recruits was reduced, in response to iron additions, with survival of recruits in iron-enriched plots doubled over that of recruits in control plots, suggests that the improved demographic status evident already after 2 years of experimental iron additions, is likely to improve even further as these vigorous recruits replace shoots produced prior to iron additions.

*P. oceanica* shoot population responses to iron additions, however, exhibited large variability. The

high variance in the responses of *P. oceanica* population dynamics to iron additions was due to the slow population dynamics of *P. oceanica*, and, to some extent, to the spatial heterogeneity of seagrass meadows. *P. oceanica* rhizomes produce 0.82 new shoots per year (Marbà and others 1996), preventing detection of clear responses of shoot recruitment to environmental change at time scales shorter than a few years. In addition, because of the slow shoot turnover time for this population ( $23 \pm 8$  years), the structure of the meadow 2 years after iron additions was similar to that in control plots because most ( $78 \pm 9\%$ ) shoots in the population receiving iron were born prior to iron additions, and hence not sensitive to iron additions. Moreover, shoot density is highly heterogeneous in *P. oceanica* meadows. Given the net population growth rates during the experiment and shoot densities at the beginning of the experiment, differences in population structure (that is, shoot density) between control and fertilized plots are expected to be significant no earlier than after 5 years of iron additions. Hence, demographic responses are projected to display their full expression in decades, which defies the logistic demands of underwater experimental ecology.

The observation that iron additions can improve the status of impacted seagrass meadows growing in carbonate sediments is, however, an important one. Mediterranean *P. oceanica* meadows are declining at rates in excess of  $5\% \text{ y}^{-1}$  across the Mediterranean basin (Marbà and others 2005), and represent, therefore, the most threatened habitats in the Mediterranean Sea. All attempts to reverse this decline have failed to date, both at the regional and even local scales. For instance, removal of a fish farm following the observation of negative impacts on the adjacent seagrass meadows (Delgado and others 1999) failed to stop the decline of the affected *P. oceanica* meadow, which continued to decline years after the farming operation was discontinued (Delgado and others 1999). The demonstration that iron additions to organic-impacted seagrass sediments can reverse seagrass decline provided here represents, therefore, an important finding pointing to avenues to reverse this process, which is depleting seagrass ecosystems in the Mediterranean and globally (Duarte and others 2002; Orth and others 2006). Whether iron additions can be safely applied at the ecosystem scale remains to be assessed, but the fact that iron addition experiments have already been conducted, for scientific purposes, rather than to restore threatened ecosystems, at a large scale over the ocean suggests that it must be feasible.

In summary, this research shows, for the first time, that seagrass decline can be reversed by iron additions. We achieved this by targeting critical nodes controlling the functioning of the system, based on previous research aimed at elucidating the demographic decline of the seagrass meadow (Marbà and others 2002, 2005), and the role of iron in promoting seagrass growth (Duarte and others 1995; Chambers and others 2001) and controlling sulfide dynamics (Holmer and others 2003, 2005) in carbonate sediments. Because iron deficiency is widespread in carbonate sediments across the ocean (Duarte and others 1995), the role of iron additions in reversing seagrass decline in this study may well apply to seagrass decline caused by organic inputs to carbonate sediments elsewhere. As seagrass meadows are suffering a global decline (Duarte 2002; Orth and others 2006), the results presented here offer an encouraging model to develop effective strategies, together with regulatory measures to reduce nutrient and organic matter inputs, to reverse decline and preserve seagrass meadows.

#### ACKNOWLEDGEMENTS

This study was funded by the EU project MedVeg (Q5RS-2001-02456) and the project 055/2002 of the Spanish Ministry of Environment. We thank the company JAER for supplying the Fe-chelate used in the experiment. We are grateful to the officers and guards of Cabrera Archipelago National Park for providing access to the study site and park facilities, and to Miguel Angel for his delicious cooking. We are indebted to Rocío Santiago and Regino Martínez for field and laboratory assistance. Elena Díaz-Almela and Maria Calleja were supported by PhD grants from the Balearic Government and the Spanish Research Council, respectively. We thank Antonio Tovar-Sánchez and two anonymous reviewers for useful comments on the manuscript.

#### REFERENCES

- Berner RA. 1984. Sedimentary pyrite formation: an update. *Geochim Cosmochim Acta* 48:605–15.
- Borum J, Sand-Jensen K, Binzer T, Pedersen O, Greve TM (2006) Oxygen movement in seagrasses. In: Larkum AWD, Orth RJ, Duarte CM (eds) *Seagrasses: Biology, Ecology and Conservation*. Dordrecht, Springer.
- Chambers RA, Fourqurean JW, Macko SA, Hoppenot R. 2001. Biogeochemical effects of iron availability on primary producers in a shallow marine carbonate environment. *Limnol Oceanogr* 46:1278–86.
- Cline JD. 1969. Spectrophotometric determination of hydrogen sulfide in natural waters. *Limnol Oceanogr* 14:454–58.
- Delgado O, Ruiz J, Pérez M, Romero J, Ballesteros E. 1999. Effects of fish farming on seagrass (*Posidonia oceanica*) in a Mediterranean bay: seagrass decline after organic loading cessation. *Oceanologia Acta* 22:109–17.
- Duarte CM. 1995. Submerged aquatic vegetation in relation to different nutrient regimes. *Ophelia* 41:87–112.
- Duarte CM. 2002. The future of seagrass meadows. *Environ Conserv* 29:192–206.
- Duarte CM, Marbà N, Agawin N, Cebrián J, Enríquez S, Fortes MD, Gallegos ME, Merino M, Olesen B, Sand-Jensen K, Uri J, Vermaat J. 1994. Reconstruction of seagrass dynamics: age determinations and associated tools for the seagrass ecologist. *Mar Ecol Prog Ser* 107:195–209.
- Duarte CM, Merino M, Gallegos M. 1995. Evidence of iron deficiency in seagrasses growing above carbonate sediments. *Limnol Oceanogr* 40:1153–58.
- Duarte CM, Borum J, Short FT, Walter DI. 2005. Seagrass ecosystems: their global status and prospects. In: Polunin NVC, Ed. *Aquatic ecosystems: trends and global prospects*. London: Cambridge University Press.
- Fossing Jørgensen H. BB. 1989. Measurement of bacterial sulfate reduction in sediments: Evaluation of a single-step chromium reduction method. *Biogeochemistry* 8:205–22.
- Green EP, Short FT. 2003. *World atlas of seagrasses*. Berkeley: University of California Press, p 286pp.
- Holmer M, Duarte CM, Marbà N. 2003. Fast sulfur turnover in carbonate seagrass (*Posidonia oceanica*) sediments. *Biogeochemistry*. 66:223–39.
- Holmer M, Duarte CM, Boschker HTS, Barron C. 2004. Carbon cycling and bacterial carbon sources in pristine and impacted Mediterranean seagrass sediments. *Aquat Microb Ecol* 36:227–37.
- Holmer M, Duarte CM, Marbà N. 2005. Iron additions improve seagrass growth on impacted carbonate sediments. *Ecosystems* 8:721–30.
- Jørgensen BB. 1978. A comparison of methods for the quantification of bacterial sulfate reduction in coastal marine sediments. *Geomicrob J* 1:11–27.
- Marbà N, Duarte CM. 1998. Rhizome elongation and seagrass clonal growth. *Mar Ecol Prog Ser* 174:269–80.
- Marbà N, Duarte CM, Cebrián J, Enríquez E, Gallegos ME, Olesen B, Sand-Jensen K. 1996. Growth and population dynamics of *Posidonia oceanica* in the Spanish Mediterranean coast: elucidating seagrass decline. *Mar Ecol Prog Ser* 137:203–13.
- Marbà N, Duarte CM, Holmer M, Martínez R, Basterretxea G, Orfica A, Jordi A, Tintoré J. 2002. Assessing the effectiveness of protection on *Posidonia oceanica* populations in the Cabrera National Park (Spain). *Environ Conserv* 29:509–18.
- Marbà N, Duarte CM, Díaz-Almela E, Terrados J, Álvarez E, Martínez R, Santiago R, Gacia E, Grau AM. 2005. Direct evidence of imbalanced seagrass (*Posidonia oceanica*) shoot population dynamics along the Spanish Mediterranean. *Estuaries* 28:51–60.
- Orth RJ, Carruthers TJB, Dennison WC, Duarte CM, Fourqurean JW, Heck KL Jr, Hughes AR, Kendrick GA, Kenworthy WJ, Olyrnik S, Short FT, Waycott M, Williams SL. 2006. A global crisis for seagrass ecosystems. *BioScience* 56:987–996.
- Pergent G, Ben Maiz N, Boudouresque CF, Meinesz A. 1989. The flowering of *Posidonia oceanica* over the past fifty years: a lepidochronological study. In: Boudouresque CF, Meinesz A,

- Fresi E, Gravez , Eds. International Workshop on Posidonia beds. vol 2 France: G.I.S. Posidonie publications. pp 69–76.
- Short FT, Duarte CM. 2001. Methods for the measurement of seagrass growth and production. In: Short FT, Coles RG, Eds. Global seagrass research methods. Amsterdam: Elsevier. pp 155–82.
- Stookey LL.. 1970. Ferrozine: a new spectrophotometric reagent for iron. *Anal Chem* 42:779–81.
- Tabatabai. 1974. Turbidimetric sulfate analyses. *Sulfur Inst J* 10:11–3.
- Terrados J, Duarte CM, Kamp-Nielsen L, Borum J, Agawin NSR, Fortes MD, Gacia E, Lacap D, Lubanski M, Greve T. 1999. Are seagrass growth and survival affected by reducing conditions in the sediment?. *Aquat Bot* 65:175–97.